method[10] and the core AO set taken from Huzinaga's (9s6p)/[3s2p] basis.[9] Tables V–VII show the comparative results for MoO_3S^{2-}. The analyses are the same as those in Tables II–IV.

The Mo chemical shift of MoO_3S^{2-} is 683 ppm by the ECP approximation and 591 ppm by the AE calculation in comparison with the experimental value 497 ppm. The error is 92 ppm in which 43 ppm is due to σ^{dia} and 49 ppm to σ^{para}. In σ^{dia}, the error is entirely due to the sulfur ligand contribution σ_s in eq 3. In σ^{para}, the error is included in the Mo p and d AO contributions. Though the AE calculation gives a better agreement with the experimental value, the error, 92 ppm, is small in comparison with the range of the chemical shifts, ~3000 ppm, studied in this paper. We therefore conclude that the ECP approximation adopted here causes little effect on the results of the present study.

Contribution from the Department of Chemistry,
Purdue University, West Lafayette, Indiana 47907

Kinetics of Oxidation of Tetracyanonickelate(II) by Chlorine Monoxide, Chlorine, and Hypochlorous Acid and Kinetics of Chlorine Monoxide Formation

Mark W. Beach and Dale W. Margerum*

Received August 15, 1989

Oxidation of $Ni^{II}(CN)_4^{2-}$ by aqueous chlorine proceeds by three parallel pathways via Cl_2O, Cl_2, and HOCl to yield *trans*-$Ni^{III}(CN)_4(H_2O)_2^-$: $d[Ni(III)]/dt = 2(k_{Cl_2O}[Cl_2O] + k_{Cl_2}[Cl_2] + k_{HOCl}[HOCl])[Ni^{II}(CN)_4^{2-}]$. The values of the second-order rate constants ($M^{-1}\ s^{-1}$; 25.0 °C; $\mu = 0.10$ M) for oxidations by Cl_2O, Cl_2, and HOCl are 1.3×10^7, 3.2×10^5, and 0.5, respectively. The proposed mechanism involves the formation of a nickel(IV) intermediate by Cl^+ transfer to nickel(II) in the rate-determining step. This is followed by a rapid electron transfer between the nickel(IV) intermediate and $Ni^{II}(CN)_4^{2-}$ to give the final nickel(III) product. When the Cl_2O path predominates and higher concentrations of $Ni^{II}(CN)_4^{2-}$ are used, the formation of Cl_2O (catalyzed by acetic acid) becomes rate limiting: $d[Cl_2O]/dt = (k_2 + k_5[HOAc])[HOCl]^2$ where k_2 is 0.12 $M^{-1}\ s^{-1}$ and k_5 is 280 $M^{-2}\ s^{-1}$. Under these conditions the direct HOCl oxidation of $Ni^{II}(CN)_4^{2-}$ also contributes to the appearance of nickel(III).

Introduction

trans-$Ni^{III}(CN)_4(H_2O)_2^-$ can be formed by either chemical or electrochemical oxidation of $Ni^{II}(CN)_4^{2-}$ in aqueous solution.[1] The Ni(III) complex is more stable in acidic than in basic solution. However, its rate of decomposition in acid increases in the presence of HCN,[2] and the HCN concentration in turn depends on the rate of dissociation[3,4] of $Ni^{II}(CN)_4^{2-}$. Hence, the rate of decomposition of Ni(III) depends on the efficiency of the $Ni^{II}(CN)_4^{2-}$ oxidation. Electrochemical oxidation using bulk electrolysis gives poor oxidation efficiency (≃50%). In contrast, chemical oxidation using aqueous chlorine[2] gives quantitative oxidation of Ni(II) to Ni(III), and it also destroys any free HCN or CN^- in the solution.[5,6]

A variety of oxidation reactions between metal–ligand complexes and chlorine species have been studied[7–9] and reviewed.[10] Part of the focus of these studies was to determine whether the mechanism involved a one- or two-electron oxidation. One such study is the oxidation of $Pt^{II}(CN)_4^{2-}$ by chlorine (Cl_2) and by hypochlorous acid (HOCl) to form the platinum(IV) complexes in eqs 1 and 2, where the value of k_{Cl_2} is 1.08×10^7 $M^{-1}\ s^{-1}$ and

$$Pt^{II}(CN)_4^{2-} + Cl_2 \xrightarrow[H_2O]{k_{Cl_2}} trans\text{-}Pt^{IV}(CN)_4(Cl)(H_2O)^- + Cl^- \tag{1}$$

$$Pt^{II}(CN)_4^{2-} + HOCl \xrightarrow[H_2O]{k_{HOCl}} trans\text{-}Pt^{IV}(CN)_4(OH)_2^{2-} + H^+ + Cl^- \tag{2}$$

the value of k_{HOCl} is 97.9 $M^{-1}\ s^{-1}$ ($\mu = 1.0$ M at 25.0 °C).[9] Since $Pt^{II}(CN)_4^{2-}$ and $Ni^{II}(CN)_4^{2-}$ are similar low-spin d^8 complexes, it is of interest to compare the oxidation kinetics of their reactions with Cl_2 and HOCl. In the present work, we find that chlorine monoxide (Cl_2O) is even more effective than Cl_2 or HOCl in the oxidation of $Ni^{II}(CN)_4^{2-}$ to *trans*-$Ni^{III}(CN)_4(H_2O)_2^-$, and three parallel paths occur (eq 3). The reaction rates are first order

$$\begin{array}{lcr} & Cl_2O \longrightarrow & Cl^- + OCl^- \\ 2Ni^{II}(CN)_4^{2-} + 2H_2O + & Cl_2 \longrightarrow & 2Ni^{III}(CN)_4(H_2O)_2^- + 2Cl^- \\ & HOCl \longrightarrow & Cl^- + OH^- \end{array} \tag{3}$$

in $Ni^{II}(CN)_4^{2-}$ and first order in each of the chlorine species. The pathway that predominates depends on the concentration of chlorine species, the Cl^- concentration, and the solution acidity. In the proposed mechanism, all three pathways involve a two-step process with formation of a highly reactive intermediate in the rate-determining step. This intermediate may be either a nickel(IV) complex or a $^{\bullet}Cl$ radical. However, thermodynamic considerations and the similarity of the kinetic results to those of an analogous study of $Pt^{II}(CN)_4^{2-}$ oxidation suggest that the nickel(IV) intermediate is more probable.

Chlorine Equilibria. The major equilibria of aqueous chlorine species are given in eqs 4–6. The decomposition reactions of OCl^- and HOCl to form ClO_2^-, ClO_3^-, and Cl^- are too slow[11,12] to interfere with studies of the $Ni^{II}(CN)_4^{2-}$ and aqueous chlorine reactions.

$$HOCl \rightleftharpoons OCl^- + H^+ \qquad pK_a = 7.5 \tag{4}$$

$$Cl_2 + H_2O \underset{k_{-1}}{\overset{k_1}{\rightleftharpoons}} HOCl + H^+ + Cl^- \qquad K_1 = 7.2 \times 10^{-4}\ M^2 \tag{5}$$

$$2HOCl \underset{k_{-2}}{\overset{k_2}{\rightleftharpoons}} Cl_2O + H_2O \qquad K_2 = 1.15 \times 10^{-2}\ M^{-1} \tag{6}$$

The pK_a value for the dissociation of HOCl is 7.5 ($\mu = 0$ M at 25 °C).[13] Equation 5 has been investigated in detail by using relaxation,[14] stopped-flow,[9] and continuous-flow techniques.[15,16]

---

(1) Pappenhagen, T. L.; Margerum, D. W. *J. Am. Chem. Soc.* **1985**, *107*, 4576–4577.
(2) Wang, Y. L.; Beach, M. W.; Pappenhagen, T. L.; Margerum, D. W. *Inorg. Chem.* **1988**, *27*, 4464–4472.
(3) Kolski, G. B.; Margerum, D. W. *Inorg. Chem.* **1968**, *7*, 2239–2243.
(4) Crouse, W. C.; Margerum, D. W. *Inorg. Chem.* **1974**, *13*, 1437–1443.
(5) Eden, E. G.; Hampson, B. L.; Wheatland, A. B. *J. Soc. Chem. Ind., London* **1950**, *69*, 244–249.
(6) Gerritsen, C. M.; Margerum, D. W. *Inorg. Chem.*, submitted for publication.
(7) Thompson, R. C.; Gordon, G. *Inorg. Chem.* **1966**, *5*, 562–569.
(8) Ondrus, M. G.; Gordon, G. *Inorg. Chem.* **1971**, *10*, 474–477.
(9) Drougge, L.; Elding, L. I. *Inorg. Chem.* **1985**, *24*, 2292–2297.
(10) Thompson, R. C. *Adv. Inorg. Bioinorg. Mech.* **1986**, *4*, 65–106.
(11) Lister, M. W. *Can. J. Chem.* **1956**, *30*, 465–478.
(12) Lister, M. W. *Can. J. Chem.* **1952**, *30*, 879–889.
(13) Morris, C. J. *J. Phys. Chem.* **1966**, *70*, 3798–3805.

0020-1669/90/1329-1225$02.50/0

The values of k_1, k_{-1}, and K_1 are 11.0 s^{-1}, 1.80 × 10^4 M^{-2} s^{-1}, and 6.0 × 10^{-4} M^2, respectively (20 °C; μ = 0.1 M).[14] The K_1 value adjusted to 25 °C is 7.2 × 10^{-4} M^2 (μ = 0.1 M), which is calculated from $\Delta H°$ = 5.06 kcal mol^{-1}.[17] The reactions in eq 5 are catalyzed by buffers (HA/A^-) such as acetate,[15] monochloroacetate, and phosphate[16] (eq 7). For acetate buffer, k_3 is

$$\mathrm{Cl_2 + A^- + H_2O \underset{k_{-3}}{\overset{k_3}{\rightleftharpoons}} HOCl + HA + Cl^-} \tag{7}$$

5.55 × 10^2 M^{-1} s^{-1} (9.5 °C, μ = 0.1 M).[15] We calculate a k_{-3} value of 40 M^{-2} s^{-1} at this temperature based on K_1 = 3.2 × 10^{-4} M^2 at 9.5 °C[14,17] and the pK_a value for acetic acid (4.56), which is almost temperature independent.[18a] Unfortunately, the activation parameters for the rate constants are not known.

The properties of Cl_2O and its formation have been reviewed.[19,20] The equilibrium constant K_2 is 3.55 × 10^{-3} M^{-1} at 0 °C and 8.70 × 10^{-3} at 19 °C as determined by Roth.[21] We estimate a value of K_2 = 1.15 × 10^{-2} M^{-1} at 25 °C by use of Roth's value for the heat of solution of Cl_2O (i.e. $\Delta H°$ = 8.0 kcal mol^{-1} for K_2).[19] The chlorination reaction of anisole by Cl_2O in acid has been used to measure the rate of Cl_2O formation, which proceeded by eq 6 and by an acid-catalyzed pathway (eq 8).[22] The values of k_2 and k_4

$$\mathrm{2HOCl + H_3O^+ \underset{k_{-4}}{\overset{k_4}{\rightleftharpoons}} Cl_2O + H_2O + H_3O^+} \tag{8}$$

were reported to be 0.124 M^{-1} s^{-1} and 3.1 M^{-2} s^{-1}, respectively (μ = 0.6 M at 25 °C).[22] The kinetics of Cl_2O formation also have been investigated in the chlorination reaction of allyl alcohol in acetate buffer.[23] It was proposed that Cl_2O formation proceeded by eq 6 and by an acetic acid catalyzed pathway (eq 9). The evaluated rate constants (μ = 0 M at 25 °C) were 0.14 M^{-1} s^{-1} for k_2 and 26 M^{-2} s^{-1} for k_5.[23]

$$\mathrm{2HOCl + HOAc \underset{k_{-5}}{\overset{k_5}{\rightleftharpoons}} Cl_2O + H_2O + HOAc} \tag{9}$$

In the present work, we reexamine the kinetics of Cl_2O formation in eqs 6 and 9 by observing the oxidation of $Ni^{II}(CN)_4^{2-}$. At higher $Ni^{II}(CN)_4^{2-}$ and HOCl concentrations and with low acetic acid concentrations, Cl_2O formation is the rate-determining step in the oxidation of $Ni^{II}(CN)_4^{2-}$ by Cl_2O. The direct oxidation of $Ni^{II}(CN)_4^{2-}$ by HOCl is also observed under these conditions.

Experimental Section

Chemicals and Solutions. Crystalline $K_2Ni^{II}(CN)_4$ and $Na_2Ni^{II}(CN)_4$ were prepared as described previously.[24] Solutions of $Ni^{II}(CN)_4^{2-}$ were prepared by dilution of these salts in 0.1 M $NaClO_4$ at pH 8. The concentration of $Ni^{II}(CN)_4^{2-}$ was determined spectrophotometrically on the basis of known molar absorptivities (ϵ_{267} = 1.16 × 10^4 M^{-1} cm^{-1}, ϵ_{285} = 4630 M^{-1} cm^{-1}, ϵ_{310} = 750 M^{-1} cm^{-1}).[4]

Solutions of OCl^- were prepared by bubbling Cl_2 gas (Matheson, ultrahigh purity, 99.9%) through ice-cooled 0.5–1 M NaOH, and for these solutions

$$\mathrm{Cl_2 + 2OH^- \rightarrow OCl^- + Cl^- + H_2O}$$

$[Cl^-] = [OCl^-]$. The absorbance at 292 nm (ϵ = 350 M^{-1} cm^{-1}) was used to determine the concentration of OCl^-. All stock solutions were protected from room light and refrigerated. These solutions were used within 1–2 weeks of preparation to minimize the degree of contamination due to OCl^- disproportionation products.[11]

Table I. Kinetic Data for the Reaction between Cl_2 and $Ni^{II}(CN)_4^{2-}$ [a]

$10^4[Cl_2]_T$, M	k_{obsd}, s^{-1} [b]	$10^4[Cl_2]_T$, M	k_{obsd}, s^{-1} [b]
0.76	60 ± 3	2.8	190 ± 10
1.5	110 ± 2	3.3	240 ± 10
2.2	150 ± 10		

[a] $[Cl^-]$ = 6.21 × 10^{-2} M; $[H^+]$ = 0.255 M; $[Ni^{II}(CN)_4^{2-}]$ = 7.2 × 10^{-6} M; μ = 1.0 M ($NaClO_4$); 25.0 ± 0.1 °C. [b] Experimental rate constants (k'_{obsd}) were corrected for mixing effects, $k_{obsd} = k'_{obsd}/[1 - (k'_{obsd}/k_m)]$, where k_m is 1700 s^{-1} for the Dionex-Durrum stopped-flow instrument: Dickson, P. N.; Margerum, D. W. *Anal. Chem.* **1986**, *58*, 3153–3158).

Chloride-free solutions of OCl^- were prepared with the procedure developed by Cady.[25] Chlorine monoxide is produced by the reaction of mercuric oxide with chlorine dissolved in CCl_4, and HOCl is formed by extracting the Cl_2O solution with water. Immediate addition of 0.5 M NaOH converted the HOCl to the more stable OCl^- for storage.

Solutions of HOCl were prepared by dilution of OCl^- solutions into buffered or $HClO_4$ media. Buffered solutions were prepared from either CH_3COONa or Na_2HPO_4 and dilute $HClO_4$. HOCl solutions were used immediately after preparation.

Solutions of Cl_2 were prepared by dilution of OCl^- into $HClO_4$ media that contained added Cl^-. Under these conditions, the principal chlorine species is Cl_2 as shown in eq 5. The Cl^- concentration was kept low enough to prevent appreciable formation of Cl_3^-.[26]

Analytical Methods. The concentration of HOCl was measured spectrophotometrically after addition of excess KI to a diluted sample of HOCl and subsequent measurement of the oxidation product I_3^- (ϵ_{353} = 26 400 M^{-1} cm^{-1}). For solutions of Cl_2, the concentration of Cl_2 was determined by a similar method, and precautions were taken to avoid Cl_2 loss due to its high volatility. The stop syringe of the stopped-flow apparatus was calibrated and used to measure aliquots of the Cl_2 solutions. The aliquots were delivered directly into a KI solution (pH 5; $[acetate]_T$ = 0.1 M).

The ionic strength for all experiments was controlled with recrystallized $NaClO_4$. Stock $HClO_4$ solutions were standardized with a NaOH solution that in turn was standardized with potassium hydrogen phthalate. Either a Sargent-Welch No. S-30072-15 or a Ross No. 810200 combination electrode connected to an Orion Research Model 601 Ionanalyzer was used to measure pH. These pH values were corrected to $p[H^+]$ ($= -\log [H^+]$) values with electrode parameters that were obtained from a strong-acid–base titration. Analysis of the titration data by the method of Gran[27] was followed by a linear regression of measured pH and $p[H^+]$ values.

UV–vis spectral data were obtained at 25.0 ± 0.1 °C with a Perkin-Elmer Model 320 spectrophotometer with a Perkin-Elmer Model 3600 data station. A spectrum of a blank of the appropriate media composition was stored in memory and automatically subtracted for all scans.

Kinetic Measurements. Reactions were followed with either a Dionex-Durrum Model D-110 or a Hi-Tech Scientific Model SFL-43 stopped-flow spectrophotometer. Both stopped-flow systems were interfaced to a Zenith 151 CPU with a Metrabyte DASH-16 A/D interface card. The Hi-Tech stopped-flow instrument was equipped with a specially designed ball-type mixing–observation cell with a 1.6-cm cell path.[28] All kinetic measurements were made at 25.0 ± 0.1 °C. For determinations of the rate constants with Cl_2 and Cl_2O, the reactions were studied under pseudo-first-order conditions with $HOCl/Cl_2$ in at least 10-fold excess over $Ni^{II}(CN)_4^{2-}$.

The method of initial rates was employed for the determination of the rate constants for Cl_2O formation and the rate constant for the HOCl pathway. Only the first 2–10% of the reaction absorbance change was used for these measurements. The reactions were studied in the presence of acetate buffer from $p[H^+]$ 4.5 to 5.1. Conditions were adjusted with high concentrations of $Ni^{II}(CN)_4^{2-}$ so that $k_{Cl_2O}[Ni^{II}(CN)_4^{2-}] \gg (k_{-2} + k_{-5}[HOAc])$. This makes formation of Cl_2O the rate-determining step. The oxidation of $Ni^{II}(CN)_4^{2-}$ serves as a scavenger for the Cl_2O formed in eq 6 and 9, so that this path is zero order in $Ni^{II}(CN)_4^{2-}$. However, direct oxidation of $Ni^{II}(CN)_4^{2-}$ by HOCl also becomes significant under

---

(14) Eigen, M.; Kustin, K. *J. Am. Chem. Soc.* **1962**, *84*, 1355–1361.

(15) Lifshitz, A.; Perlmutter-Hayman, B. J. *J. Phys. Chem.* **1961**, *65*, 753–757.

(16) Lifshitz, A.; Perlmutter-Hayman, B. J. *J. Phys. Chem.* **1962**, *66*, 701–705.

(17) Connick, R. E.; Yuan-Tsan, C. *J. Am. Chem. Soc.* **1959**, *81*, 1280–1284.

(18) (a) Martell, A. E.; Smith, R. M. *Critical Stability Constants*; Plenum Press: New York, 1977; Vol. 3. (b) *Ibid.* 1976; Vol. 4.

(19) Renard, J. J.; Boker, H. I. *Chem. Rev.* **1976**, *76*, 487–508.

(20) Wojtowicz, J. A. In *Kirk-Othmer Encyclopedia of Chemical Technology*, 3rd ed.; Interscience: New York, 1980.

(21) Roth, W. A. *Z. Phys. Chem. Abt. A* **1929**, *145*, 289–297.

(22) Swain, C. G.; Crist, D. R. *J. Am. Chem. Soc.* **1972**, *94*, 3195–3200.

(23) Israel, G. C. *J. Chem. Soc.* **1950**, 1286–1289.

(24) Fernelius, W. C., Ed. *Inorganic Synthesis*; McGraw Hill: New York, 1946, Vol. 2, pp 227–228.

(25) Cady, G. H. *Inorg. Synth.* **1957**, *5*, 156–165.

(26) Zimmerman, G.; Strong, C. F. *J. Am. Chem. Soc.* **1957**, *79*, 2063–2066.

(27) Rossotti, F. J.; Rossotti, H. J. *J. Chem. Educ.* **1965**, *42*, 375–378.

(28) Wang, Y. L. Ph.D. Thesis, Purdue University, 1989.

Table II. Rate Constants for the Determination of the Cl_2O Pathway for Oxidation of $Ni^{II}(CN)_4^{2-}$ [a]

10^4[HOCl], M	k_{obsd}, s^{-1}	10^4[HOCl], M	k_{obsd}, s^{-1}
HOCl Solutions at $p[H^+]$ 5.0 with $[Cl^-]_i \simeq 0$ M[b]			
4.18	0.054 ± 0.001	25.6	2.0 ± 0.1
8.30	0.228 ± 0.005		
HOCl Solutions at $p[H^+]$ 5.0 with $[Cl^-] \simeq$ [HOCl][c]			
2.09	0.017 ± 0.001	26.0	2.06 ± 0.04
5.71	0.087 ± 0.002	35.2	3.5 ± 0.1
13.2	0.467 ± 0.004		
HOCl Solutions at $p[H^+]$ 5.9–6.1 with $[Cl^-] \simeq$ [HOCl][d]			
3.55	0.035 ± 0.001	13.9	0.497 ± 0.003
4.86	0.069 ± 0.003	28.7	2.49 ± 0.05
6.90	0.118 ± 0.004		

[a] $\mu = 0.10$ M ($NaClO_4$) at 25.0 ± 0.1 °C. [b] $[acetate]_T = 0.042$ M; $[Ni^{II}(CN)_4^{2-}] = 4.0 \times 10^{-6}$ M. [c] $[acetate]_T = 0.042$ M; $[Ni^{II}(CN)_4^{2-}] = 1.5 \times 10^{-5}$ M. [d] $[phosphate]_T = 0.013–0.023$ M; $[Ni^{II}(CN)_4^{2-}] = (5.6–7.0) \times 10^{-6}$ M.

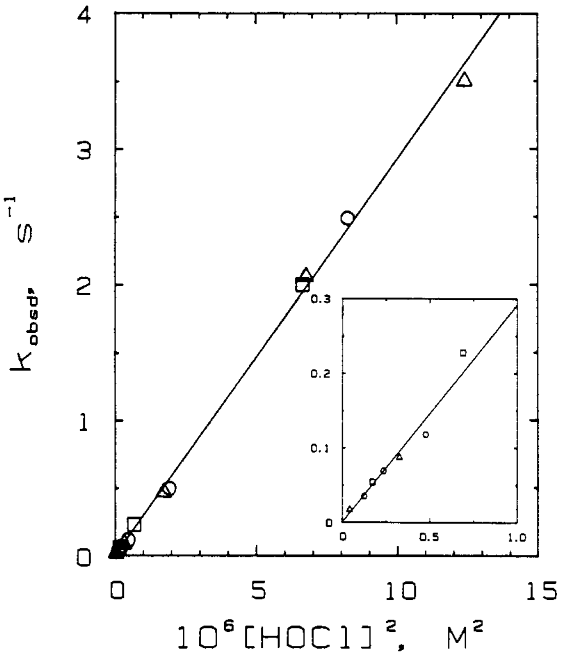

Figure 1. Pseudo-first-order rate constants for the reaction between Cl_2O and $Ni^{II}(CN)_4^{2-}$: (△) $[Cl^-] \simeq$ [HOCl], $p[H^+]$ 5.0; (○) $[Cl^-] \simeq$ [HOCl], $p[H^+]$ 5.9–6.1; (□) $[Cl^-]_i \simeq 0$ M, $p[H^+]$ 5.0.

these conditions, and the overall reaction is intermediate between zero and first order in $Ni^{II}(CN)_4^{2-}$.

The reactions were followed by monitoring the formation of $Ni^{III}(CN)_4(H_2O)_2^-$ at either 234 or 250 nm ($\epsilon_{234} = 8.02 \times 10^3$ M^{-1} cm^{-1}, $\epsilon_{250} = 1.15 \times 10^4$ M^{-1} cm^{-1}).[2] The tabulated k_{obsd} and initial rate (V_i) values are averages of three to six trials, and uncertainties are reported for 1 standard deviation.

Results and Discussion

Cl_2 Pathway: Determination of k_{Cl_2}. The kinetics of the reaction of $Ni^{II}(CN)_4^{2-}$ with excess chlorine (0.76×10^{-4} to 3.3×10^{-4} M) were studied at $[H^+] = 0.255$ M and $[Cl^-] = 6.21 \times 10^{-2}$ M (Table I). At $\mu = 1.0$ M and 25.0 °C, K_1 is 3.27×10^{-4} M^2 for eq 5, which indicates 97% of the total active chlorine is present as Cl_2.[9] Individual reactions give excellent first-order plots, and the k_{obsd} values are directly proportional to $[Cl_2]$ (Table I). The experimentally determined rate expression is given in eq 10, where $k_{Cl_2} = (3.6 \pm 0.1) \times 10^5$ M^{-1} s^{-1}.

$$\frac{d[Ni(III)]}{dt} = 2k_{Cl_2}[Cl_2][Ni^{II}(CN)_4^{2-}] \qquad (10)$$

Cl_2O Pathway: Determination of k_{Cl_2O}. The reaction of excess HOCl with $Ni^{II}(CN)_4^{2-}$ ($p[H^+]$ 5.0–6.1; $\mu = 0.10$ M) gives excellent first-order plots. The reaction was studied under conditions where $[Cl^-]_i \simeq 0$ M and where $[Cl^-] \simeq$ [HOCl] (Table II). All sets of data give the same $[HOCl]^2$ dependence (Figure 1), which denotes a negligible Cl^- dependence for the reaction from $[Cl^-] = 2 \times 10^{-4}$ to 35×10^{-4} M. There is also no H^+ dependence from $p[H^+]$ 5.0 to 6.1. At the highest $[Cl^-]$ (35×10^{-4} M) for data in Table II, the calculated contribution for Cl_2 oxidation of $Ni^{II}(CN)_4^{2-}$ is only 3%. Thus, oxidation of $Ni^{II}(CN)_4^{2-}$ by the Cl_2 pathway is not significant under these conditions. The $[HOCl]^2$ dependence also is not caused by ClO_2^- oxidation of $Ni^{II}(CN)_4^{2-}$, where ClO_2^- is formed by the disproportionation of HOCl:[12]

Table III. Dependence of k_{obsd} on Chloride Concentration for the Reaction between Excess HOCl and $Ni^{II}(CN)_4^{2-}$ at $p[H^+]$ 5.1[a]

$10^3[Cl^-]$, M	k_{obsd}, s^{-1}	$10^3[Cl^-]$, M	k_{obsd}, s^{-1}
1.28	0.471 ± 0.002	20.3	0.66 ± 0.01
3.82	0.504 ± 0.004	27.5	0.73 ± 0.01
7.63	0.528 ± 0.005	33.0	0.750 ± 0.007

[a] $[acetate]_T = 0.050$ M; $[HOCl] = 1.3 \times 10^{-3}$ M; $[Ni^{II}(CN)_4^{2-}] = (4.4–14) \times 10^{-6}$ M; $\mu = 0.10$ M ($NaClO_4$); 25.0 ± 0.1 °C.

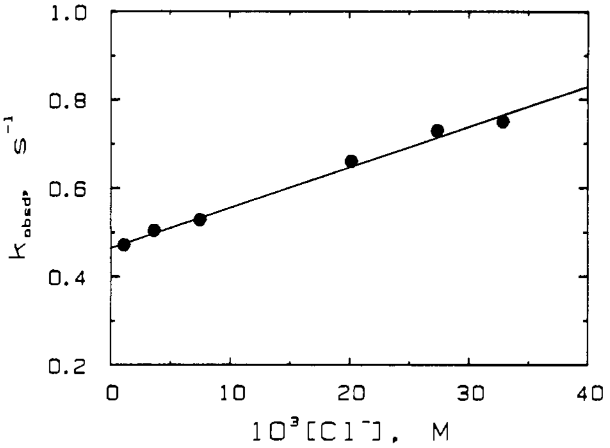

Figure 2. Dependence of k_{obsd} on chloride ion at $p[H^+]$ 5.1. The plot is a fit of eq 12 with $[HOCl] = 1.3 \times 10^{-3}$ M.

$$2HOCl \rightarrow ClO_2^- + 2H^+ + Cl^-$$

$$k_d = 7.5 \times 10^{-4}\ M^{-1}\ s^{-1}\ (30\ °C;\ \mu = 3.70\ M)$$

Formation of ClO_2^- is too slow to be a factor in the oxidation reaction of $Ni^{II}(CN)_4^{2-}$. Furthermore, direct tests indicate that ClO_2^- does not oxidize $Ni^{II}(CN)_4^{2-}$ to $Ni^{III}(CN)_4(H_2O)_2^-$ at pH 5 (acetate buffer).

A third-order oxidation reaction mechanism between two HOCl molecules and a Ni(II) complex is very unlikely. Rather, the reaction must involve a rapid preequilibrium between two HOCl molecules to form Cl_2O (eq 6). The rate expression based on this preequilibrium is given in eq 11. Equation 11 gives the necessary

$$\frac{d[Ni(III)]}{dt} = 2k_{Cl_2O}K_2[HOCl]^2[Ni^{II}(CN)_4^{2-}] \qquad (11)$$

$[HOCl]^2$ dependence (Figure 1), where $2k_{Cl_2O}K_2 = (2.93 \pm 0.03) \times 10^5$ M^{-2} s^{-1}. On the basis of $K_2 = 1.15 \times 10^{-2}$ M^{-1} and our estimate of the precision, the value of k_{Cl_2O} is $(1.3 \pm 0.1) \times 10^7$ M^{-1} s^{-1}.

At $p[H^+]$ 5.1 (acetate buffer) and in the presence of a large amount of Cl^-, Cl_2 oxidation of $Ni^{II}(CN)_4^{2-}$ becomes evident as shown by the Cl^- dependence data in Table III. The formation of Cl_2 is rapid due to catalysis by acid (eq 5) as well as acetate buffer (eq 7). The requirement for a rapid preequilibrium is met: $(k_3[OAc^-] + k_1) > k_{Cl_2}[Ni^{II}(CN)_4^{2-}]$. Thus, the overall reaction for oxidation of $Ni^{II}(CN)_4^{2-}$ under these conditions proceeds via both Cl_2O and Cl_2 pathways. Equation 12 shows the relationship

$$k_{obsd} = \frac{2k_{Cl_2}[HOCl][H^+][Cl^-]}{K_1} + 2k_{Cl_2O}K_2[HOCl]^2 \qquad (12)$$

for the k_{obsd} values plotted against $[Cl^-]$ in Figure 2, where $k_{Cl_2O} = (1.2 \pm 0.1) \times 10^7$ M^{-1} s^{-1} and $k_{Cl_2} = (3.2 \pm 0.1) \times 10^5$ M^{-1}

Table IV. Initial Rate Dependence on the Total Acetate Buffer Concentration and p[H^+] for Cl_2O Formation and HOCl Oxidation of $Ni^{II}(CN)_4^{2-}$ [a]

p[H^+]	10^4[HOCl], M	10^3[acetate]$_T$, M	10^6V_i, M s^{-1}
Buffer Dependence at [$Ni^{II}(CN)_4^{2-}$] = 8.3 × 10^{-4} M			
5.19	13.6	2.09	1.60 ± 0.05
5.09	13.6	3.14	2.0 ± 0.1
5.09	13.6	5.23	2.5 ± 0.1
5.07	13.6	6.27	2.94 ± 0.04
5.01	13.6	8.36	3.52 ± 0.02
5.01	13.6	10.4	3.94 ± 0.03
p[H^+] Dependence at [$Ni^{II}(CN)_4^{2-}$] = 6.7 × 10^{-4} M			
5.07	8.24	6.27	1.2 ± 0.2
4.77	8.24	6.27	1.6 ± 0.1
4.51	8.24	6.27	1.8 ± 0.1

[a] [Cl^-]$_i$ ≃ 0 M; μ = 0.10 M ($NaClO_4$); 25.0 ± 0.1 °C; pK_a(HOAc) = 4.56 (μ = 0.1 M at 25 °C).

Table V. Initial Rate Dependence on the Concentrations of $Ni^{II}(CN)_4^{2-}$ and HOCl for Cl_2O Formation and HOCl Oxidation of $Ni^{II}(CN)_4^{2-}$ [a]

10^4[Ni(II)], M	10^3[acetate]$_T$, M	10^4[HOCl], M	10^6V_i, M s^{-1}
HOCl Dependence at p[H^+] 5.1 with [Cl^-]$_i$ ≃ 0 M			
5.2	2.09	3.67	0.30 ± 0.02
5.2	2.09	7.95	0.71 ± 0.03
5.2	2.09	11.5	1.1 ± 0.1
5.2	2.09	21.2	3.5 ± 0.1
5.2	2.09	27.7	5.2 ± 0.1
6.7	6.27	4.86	0.62 ± 0.04
6.7	6.27	8.25	1.2 ± 0.2
6.7	6.27	28.2	9.0 ± 0.2
$Ni^{II}(CN)_4^{2-}$ Dependence at p[H^+] 5.0 with [Cl^-]$_i$ ≃ 0 M			
2.5	3.14	1.16	0.062 ± 0.006
5.0	3.14	1.16	0.09 ± 0.02
7.5	3.14	1.16	0.13 ± 0.01
HOCl Dependence at p[H^+] 5.0 with [Cl^-] ≃ [HOCl]			
3.6	2.09	3.82	0.46 ± 0.02
3.6	2.09	7.50	1.47 ± 0.05
3.6	2.09	15.8	5.9 ± 0.4
3.6	2.09	31.8	23.8 ± 0.3
HOCl Dependence at p[H^+] 4.5 with [Cl^-] ≃ [HOCl]			
1.3	2.09	3.28	0.58 ± 0.03
1.3	2.09	8.20	3.1 ± 0.1
1.3	2.09	16.6	11.6 ± 0.2
1.3	2.09	28.6	41.8 ± 0.3

[a] μ = 0.10 M ($NaClO_4$); 25.0 ± 0.1 °C.

s^{-1} (μ = 0.10 M). The k_{Cl_2O} value determined from the intercept in Figure 2 is in good agreement with the value determined from the slope of Figure 1. The k_{Cl_2} value from the slope in Figure 2 also is in good agreement with the value obtained from Table I.

Kinetics of Cl_2O Formation and Determination of k_{HOCl}. Chlorine monoxide reacts so rapidly with $Ni^{II}(CN)_4^{2-}$ that even moderate concentrations of the Ni(II) complex (>10^{-4} M) can shift the rate-determining step of the oxidation process back to the formation of Cl_2O. The H_3O^+-catalyzed pathway (eq 8) is negligible above pH 4 and the proposed mechanism is

$$2HOCl \underset{k_{-2}}{\overset{k_2}{\rightleftharpoons}} Cl_2O + H_2O$$

$$2HOCl + HOAc \underset{k_{-5}}{\overset{k_5}{\rightleftharpoons}} Cl_2O + H_2O + HOAc$$

$$Ni(II) + Cl_2O \xrightarrow{k_{Cl_2O}} \text{products: } Ni(III)$$

A steady-state approximation in terms of the Cl_2O concentration gives the rate expression in eq 13. The condition necessary to make Cl_2O formation rate determining is $k_{Cl_2O}[Ni^{II}(CN)_4^{2-}] \gg (k_{-2} + k_{-5}[HOAc])$. This leads to the rate expression in eq 14.

$$\frac{d[Ni(III)]}{dt} = \frac{2(k_2 + k_5[HOAc])[HOCl]^2 k_{Cl_2O}[Ni^{II}(CN)_4^{2-}]}{(k_{-2} + k_{-5}[HOAc]) + k_{Cl_2O}[Ni^{II}(CN)_4^{2-}]} \qquad (13)$$

$$\frac{d[Ni(III)]}{dt} = 2(k_2 + k_5[HOAc])[HOCl]^2 \qquad (14)$$

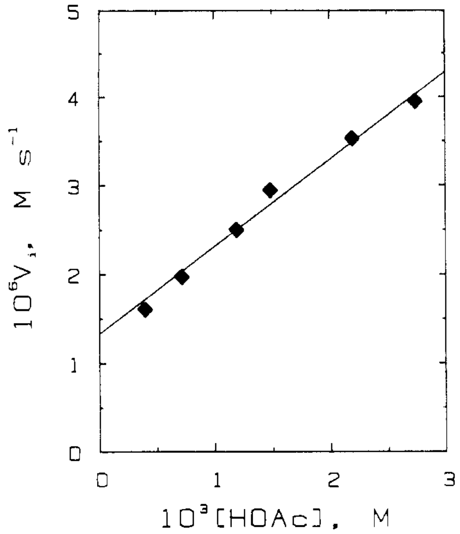

Figure 3. Dependence of initial rate (V_i) on acetic acid at p[H^+] 5.1.

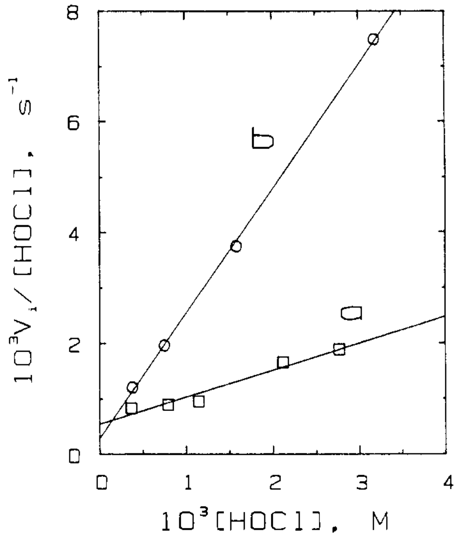

Figure 4. Effect of HOCl and Cl^- on the initial rate for Cl_2O formation and HOCl oxidation of $Ni^{II}(CN)_4^{2-}$ at [acetate]$_T$ = 2.09 mM (eq 15): (a) p[H^+] 5.1, [Cl^-]$_i$ ≃ 0 M; (b) p[H^+] 5.0, [Cl^-] ≃ [HOCl].

Tables IV and V give conditions (p[H^+] 4.5–5.2; [HOCl] = 0.12–3.2 mM; [$Ni^{II}(CN)_4^{2-}$] = 0.07–0.88 mM; [acetate]$_T$ = 2.1–10.4 mM) that indicate the initial rate measurements (V_i) depend on [HOCl]^2 and the acetic acid concentration as predicted by eq 14. However, the experimentally observed rate expression (eq 15) also has a term with a first-order dependence in [HOCl]

$$\frac{d[Ni(III)]}{dt} = 2(k_2 + k_5[HOAc])[HOCl]^2 + 2k_{HOCl}[Ni^{II}(CN)_4^{2-}][HOCl] \qquad (15)$$

and in [$Ni^{II}(CN)_4^{2-}$]. This term (with the k_{HOCl} rate constant) is attributed to the direct oxidation of $Ni^{II}(CN)_4^{2-}$ by HOCl. The observed reaction is mixed zero order and first order in Ni(II), so initial rate methods are used to resolve the rate constants. The initial rate method also enables use of higher concentrations of Ni(II) and avoids complications due to the Cl^- released in the overall reaction. The increase in rate with [H^+] at constant [acetate]$_T$ (Table IV) confirms the catalytic effect by acetic acid. The plot in Figure 3 of V_i against [HOAc] corresponds to eq 15 where the intercept is $2(k_2[HOCl]^2 + k_{HOCl}[Ni^{II}(CN)_4^{2-}][HOCl])$ and the slope is $2k_5[HOCl]^2$. Figure 4a shows a plot of V_i/[HOCl]

Table VI. Summary of Rate Constants at 25.0 °C

$Ni^{II}(CN)_4^{2-}$ Oxidation

oxidant	rate const, $M^{-1}\ s^{-1}$	conditions
Cl_2O	$(1.3 \pm 0.1) \times 10^7$	$\mu = 0.10$ M; excess HOCl; $p[H^+]$ 5.0–6.1; $K_2 = 1.15 \times 10^{-2}\ M^{-1}$
Cl_2	$(3.2 \pm 0.1) \times 10^5$	$\mu = 0.10$ M; excess HOCl; $p[H^+]$ 5.1; $[Cl^-] = 1$–33 mM
	$(3.6 \pm 0.1) \times 10^5$	$\mu = 1.0$ M; excess Cl_2; $[H^+] = 0.255$ M; $[Cl^-] = 0.0621$ M
HOCl	0.5 ± 0.1	$\mu = 0.10$ M; $p[H^+]$ 5; $[Cl^-]_i \simeq 0$ M

Cl_2O Formation

pathway	rate const	ref
H_2O	$0.08 \pm 0.04\ M^{-1}\ s^{-1}$	*a*
	$0.124 \pm 0.005\ M^{-1}\ s^{-1}$	*b*
	$0.14\ M^{-1}\ s^{-1}$	*c*
H_3O^+	$3.1 \pm 0.3\ M^{-2}\ s^{-1}$	*b*
HOAc	$280 \pm 50\ M^{-2}\ s^{-1}$	*a*

[a] This work; $[Cl^-]_i \simeq 0$ M, $\mu = 0.10$ M ($NaClO_4$). [b] Reference 22; $\mu = 0.6$ M. [c] Reference 23; $\mu = 0$ M.

against [HOCl] also in accord with eq 15, where the intercept is $2k_{HOCl}[Ni^{II}(CN)_4^{2-}]$ and the slope is $2(k_2 + k_5[HOAc])$. The rate constants k_2, k_5, and k_{HOCl} were evaluated in the following fashion from Figures 3 and 4a. First, k_5 was calculated from the slope of the buffer dependence, and k_{HOCl} was calculated from the intercept of the HOCl dependence. These values for k_5 and k_{HOCl} were used to calculate a value for k_2 from both dependencies, which was $0.08 \pm 0.04\ M^{-1}\ s^{-1}$. This is in good agreement with the value of $0.124 \pm 0.005\ M^{-1}\ s^{-1}$ determined by Swain and Crist.[22] Since their value for k_2 is more precise, it was used to recalculate k_5 from both dependencies. For k_{HOCl}, values were calculated from the same HOCl and buffer dependencies as used in the calculations for k_5. In addition, the $Ni^{II}(CN)_4^{2-}$ dependence in Table V was used because the conditions (high $[Ni^{II}(CN)_4^{2-}]$ and low [HOCl]) suggest a large contribution from the HOCl pathway. Average values were calculated from these results are $k_{HOCl} = 0.5 \pm 0.1\ M^{-1}\ s^{-1}$ and $k_5 = 280 \pm 50\ M^{-2}\ s^{-1}$, where the uncertainties for both values are estimates from the range of the individual values.

The value for k_5 is significantly higher than the value of 26 $M^{-2}\ s^{-1}$ reported by Israel.[23] Israel's value is not consistent with our results in Table II in the absence of Cl^-. We find a first-order dependence in $Ni^{II}(CN)_4^{2-}$ under these conditions, whereas his value for k_5 would predict a zero-order dependence in $Ni^{II}(CN)_4^{2-}$. Israel's determination was based on a rapid reaction of allyl alcohol with Cl_2O, where aliquots were periodically withdrawn from the reaction mixture and the HOCl concentration determined by iodometric titration. Our method involves continuous monitoring of the first 2–10% of the reaction with a stopped-flow spectrophotometer. The rate expression reported by Israel is mixed zero order and first order with respect to allyl alcohol and is similar to our rate expression in eq 15, where allyl alcohol replaces $Ni^{II}(CN)_4^{2-}$. However, the zero-order component for the rate expression proposed by Israel contains an additional term and is more complicated than our proposed expression. The aliquot method also places severe limitations as to when the first measurement can be made and a significant portion of the reaction can be missed. In our study, the method employed (stopped-flow spectroscopy and initial rates) is well suited for the measurement of rapid reaction rates. We believe our value for k_5 is more reliable since our method involves continuous monitoring and a more accurate kinetic method. Our rate constants are summarized in Table VI.

It is interesting that the acetic acid catalyzed rate for formation of Cl_2O is greater than the H_3O^+-catalyzed rate. Clearly, the effect does not follow typical general-acid catalysis based on acid strength. Two mechanisms are suggested in Scheme I. In mechanism a, acetic acid acts as a proton donor with one HOCl and a proton acceptor from another HOCl as Cl_2O is formed. In mechanism b, the catalysis is attributed to the product of $[H_3O^+][CH_3COO^-]$, which is not easily distinguished from a term in $[CH_3COOH]$. In both mechanisms the proton-transfer steps assist the formation of a new O–Cl bond as another O–Cl bond breaks. Although its effect was not explicitly studied, phosphate buffer also appears to catalyze the formation of Cl_2O. In order to have the observed contribution from Cl_2O at $p[H^+]$ 5.9–6.1 in the presence of phosphate buffer (Table II), the formation of Cl_2O must be catalyzed by the buffer.

Scheme I

mechanism a

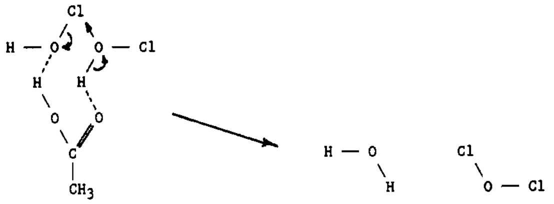

mechanism b

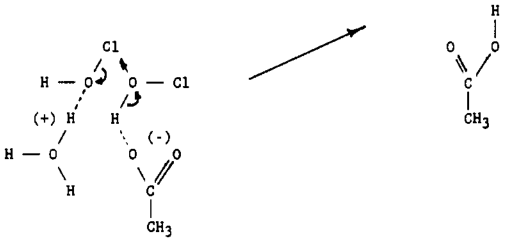

Chloride Ion Effect on Cl_2O Formation. Additional initial-rate studies at $p[H^+]$ values of 5.0 and 4.5 under conditions where $[Cl^-] \simeq [HOCl]$ are summarized in Table V. The initial rate still depends on $[HOCl]^2$, but Cl^- accelerates the reaction. Figure 4b shows an HOCl dependence at $p[H^+]$ 5.0 that fits eq 15, but the slope of this line is 4.6 times greater than that in Figure 4a, where $[Cl^-]_i \simeq 0$ M. The possibility that this Cl^- effect is due to Cl_2 formation (eqs 5 and 7) followed by Cl_2 oxidation of $Ni^{II}(CN)_4^{2-}$ can be discarded even though the rate of Cl_2 formation is the same magnitude as the rate of Cl_2O formation. Calculations show that Cl_2O oxidation of $Ni^{II}(CN)_4^{2-}$ is about 10 times faster than Cl_2 oxidation of $Ni^{II}(CN)_4^{2-}$ at $p[H^+]$ 4.50 and $[HOCl] = [Cl^-] = 2.9$ mM (the experimental conditions in Table V most favorable for a Cl_2 pathway). Hence, the oxidation of $Ni^{II}(CN)_4^{2-}$ must still be carried by the Cl_2O pathway. Another possibility is that the Cl_2O formation reactions in eqs 6 and 9 are catalyzed by Cl^-. If this were the case, the reaction should show a $[HOCl]^3$ dependence because $[Cl^-] \simeq [HOCl]$. An alternative explanation is that Cl^- reacts with HOCl to form Cl_2, which in turn reacts with HOCl to form Cl_2O in a very rapid reaction. Cl_2 formation would proceed by acid (k_{-1}) and acetic acid (k_{-3}) catalyzed pathways (eqs 5 and 7).

$$HOCl + Cl^- + H^+ \xrightarrow{k_{-1}} Cl_2 + H_2O$$

$$HOCl + Cl^- + HOAc \xrightarrow{k_{-3}} Cl_2 + OAc^- + H_2O$$

$$Cl_2 + HOCl + OAc^- \xrightarrow{\text{fast}} Cl_2O + HOAc + Cl^- \quad (16)$$

The overall rate expression based on Cl_2O formation is given in eq 17. Equation 17 simplifies to eq 18 with $[Cl^-] \simeq [HOCl]$.

$$V_i = 2(k_2[HOCl]^2 + k_5[HOCl]^2[HOAc] + k_{-1}[HOCl][Cl^-][H^+] + k_{-3}[HOCl][Cl^-][HOAc] + k_{HOCl}[HOCl][Ni^{II}(CN)_4^{2-}]) \quad (17)$$

$$V_i = 2[HOCl]^2(k_2 + k_5[HOAc] + k_{-1}[H^+] + k_{-3}[HOAc]) + 2k_{HOCl}[HOCl][Ni^{II}(CN)_4^{2-}] \quad (18)$$

For the data at $p[H^+]$ 4.5 in Table V, the contribution from the last term in eq 18 to the overall rate is negligible, which leads to eq 19. Figure 5 shows the V_i dependence on $[HOCl]^2$. By use

$$V_i = 2[HOCl]^2(k_2 + k_5[HOAc] + k_{-1}[H^+] + k_{-3}[HOAc]) \quad (19)$$

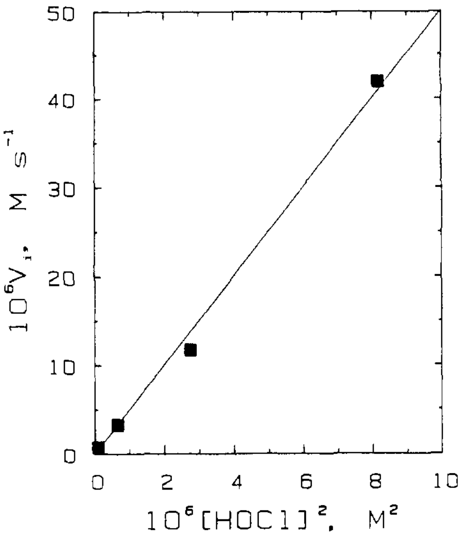

Figure 5. Effect of $[\mathrm{HOCl}]^2$ on the initial rate for $\mathrm{Cl_2O}$ formation (eq 19) with $[\mathrm{Cl^-}] \simeq [\mathrm{HOCl}]$ at $\mathrm{p[H^+]}$ 4.5.

of the previously determined values for k_2 and k_5, k_{-1} and k_{-3} are evaluated to be 3.3×10^4 $\mathrm{M^{-2}\ s^{-1}}$ and 920 $\mathrm{M^{-2}\ s^{-1}}$, respectively. The value of k_{-1} is very close to the value of 1.80×10^4 $\mathrm{M^{-2}\ s^{-1}}$ reported by Eigen and Kustin, which was determined at 20 °C ($\mu = 0.1$ M).[14] The value of k_{-3} is higher than the calculated value at 9.5 °C ($\mu = 0.1$ M) of 40 $\mathrm{M^{-2}\ s^{-1}}$. This suggests there may be a large temperature effect for the reaction in eq 7. The $\mathrm{Cl^-}$ acceleration proposed in eq 16 that leads to eq 18 is based on a fast reaction between $\mathrm{Cl_2}$ and HOCl to give $\mathrm{Cl_2O}$. To our knowledge, this reaction has not been observed previously. It seems likely that acetate ion would catalyze such a reaction in a mechanism similar to Scheme Ib. The $\mathrm{Cl^-}$ effect to give $\mathrm{Cl_2}$ and $\mathrm{Cl_2O}$ not only is needed to explain the data in Table V but also is needed to explain the preequilibrium of $\mathrm{Cl_2O}$ in Table II, when $[\mathrm{Cl^-}] \simeq [\mathrm{HOCl}]$ at $\mathrm{p[H^+]}$ 5.

Reactions with $[\mathrm{Ni^{II}(CN)_4^{2-}}] \gg [\mathrm{HOCl}]$. Attempts were made to isolate the HOCl pathway for oxidation of $\mathrm{Ni^{II}(CN)_4^{2-}}$ with higher concentrations of $\mathrm{Ni^{II}(CN)_4^{2-}}$ (>1 mM) and lower HOCl concentrations ($<1 \times 10^{-5}$ M), where the HOCl pathway should predominate. However, the reaction showed several complications under these conditions. As the $\mathrm{p[H^+]}$ increased, the extent of reaction decreased (in terms of the detectable absorbance change), whereas the rate constant for the reaction increased. We believe these effects are caused by the reaction of HOCl with trace amounts of cyanide. HOCl oxidizes $\mathrm{CN^-}$ to form CNCl (eq 20).[6]

$$\begin{gathered}\mathrm{HOCl} + \mathrm{CN^-} \rightarrow \mathrm{CNCl} + \mathrm{OH^-} \\ k = 1.2 \times 10^9\ \mathrm{M^{-1}\ s^{-1}}\ (25.0\ ^\circ\mathrm{C};\ \mu = 1.0\ \mathrm{M})\end{gathered} \tag{20}$$

The $\mathrm{p}K_\mathrm{a}$ of HCN is 9.01 at $\mu = 0.1$ M and 25 °C.[18b] Traces of cyanide form in these $\mathrm{Ni^{II}(CN)_4^{2-}}$ solutions because of the decomposition of $\mathrm{Ni^{II}(CN)_4^{2-}}$ to cyanide (eq 21). The $\mathrm{Ni^{II}(CN)_4^{2-}}$

$$\mathrm{Ni^{II}(CN)_4^{2-}} \rightarrow \mathrm{Ni^{2+}} + 4\mathrm{CN_T} \tag{21}$$

decomposition rate constant, measured in the presence of an iodine scavenger, is $k_\mathrm{d} = 4.8 \times 10^{-4}$ $\mathrm{s^{-1}}$ from pH 3 to 8.[4] Thus, only 0.5 s is required to form enough cyanide from the decomposition of 6 mM $\mathrm{Ni^{II}(CN)_4^{2-}}$ to consume 5×10^{-6} M HOCl. Another problem in studies of the reaction with excess $\mathrm{Ni^{II}(CN)_4^{2-}}$ is the formation of a product with a higher absorbance than $\mathrm{Ni^{III}(CN)_4(H_2O)_2^-}$. Frozen EPR spectra of $\mathrm{Ni^{III}(CN)_4(H_2O)_2^-}$ in the presence of excess $\mathrm{Ni^{II}(CN)_4^{2-}}$ indicate formation of a $[\mathrm{Ni^{III}(CN)_4{\cdot}Ni^{II}(CN)_4}]^{3-}$ species. We suspect that a similar species may form as a product of the reaction between excess $\mathrm{Ni^{II}(CN)_4^{2-}}$ and HOCl.

Mechanism for Ni(III) Formation. There are at least two possible mechanisms for the oxidation of $\mathrm{Ni^{II}(CN)_4^{2-}}$ by $\mathrm{Cl_2}$, $\mathrm{Cl_2O}$, and HOCl. The difference between the two mechanisms depends on whether the nickel undergoes a two- or one-electron oxidation in the rate-determining step of the reaction. A two-electron oxidation leads to formation of a Ni(IV) intermediate. A one-electron oxidation gives Ni(III) and a chlorine radical intermediate. The proposed mechanism for a two-electron reaction of the chlorine species is given in Scheme II. The final product is $\mathrm{Ni^{III}(CN)_4(H_2O)_2^-}$ for all three parallel paths. The first step of these oxidative-addition reactions with $\mathrm{Cl_2O}$ and $\mathrm{Cl_2}$ involves transfer of $\mathrm{Cl^+}$ to nickel. For HOCl, this step could involve either a $\mathrm{Cl^+}$ or $\mathrm{OH^+}$ transfer. Reactions of this type have been proposed for oxidation of Pt(II) and Pd(II) complexes by halogens.[29,30] The ion-transfer or oxidative-addition step facilitates formation of the nickel(IV) intermediate. A number of nickel(IV) complexes are known.[31,32] In particular, hexadentate bis(oxime) complexes of nickel(IV) have been well characterized.[33,34] One such complex, the hexadentate bis(oxime imine) of nickel(IV) has been observed as a product in the oxidation of its nickel(II) analogue by aqueous bromine.[35]

Scheme II. Parallel Pathways with Ni(IV) Intermediates

$\mathrm{Cl_2O}$ Reaction

$$\mathrm{Ni^{II}(CN)_4^{2-}} + \mathrm{Cl_2O} \xrightarrow[\mathrm{H_2O}]{k_{\mathrm{Cl_2O}}} \mathrm{Ni^{IV}(CN)_4(Cl)(H_2O)^-} + \mathrm{OCl^-}$$

$$\mathrm{Ni^{II}(CN)_4^{2-}} + \mathrm{Ni^{IV}(CN)_4(Cl)(H_2O)^-} \xrightarrow[\mathrm{H_2O}]{\text{fast}} 2\mathrm{Ni^{III}(CN)_4(H_2O)_2^-} + \mathrm{Cl^-}$$

$\mathrm{Cl_2}$ Reaction

$$\mathrm{Ni^{II}(CN)_4^{2-}} + \mathrm{Cl_2} \xrightarrow[\mathrm{H_2O}]{k_{\mathrm{Cl_2}}} \mathrm{Ni^{IV}(CN)_4(Cl)(H_2O)^-} + \mathrm{Cl^-}$$

$$\mathrm{Ni^{II}(CN)_4^{2-}} + \mathrm{Ni^{IV}(CN)_4(Cl)(H_2O)^-} \xrightarrow[\mathrm{H_2O}]{\text{fast}} 2\mathrm{Ni^{III}(CN)_4(H_2O)_2^-} + \mathrm{Cl^-}$$

HOCl Reaction

$$\mathrm{Ni^{II}(CN)_4^{2-}} + \mathrm{HOCl} \xrightarrow[\mathrm{H_2O}]{k_{\mathrm{HOCl}}} \begin{array}{c}\mathrm{Ni^{IV}(CN)_4(Cl)(H_2O)^-} + \mathrm{OH^-} \\ \text{or} \\ \mathrm{Ni^{IV}(CN)_4(OH)(H_2O)^-} + \mathrm{Cl^-}\end{array}$$

$$\mathrm{Ni^{II}(CN)_4^{2-}} + \begin{array}{c}\mathrm{Ni^{IV}(CN)_4(Cl)(H_2O)^-} \\ \text{or} \\ \mathrm{Ni^{IV}(CN)_4(OH)(H_2O)^-}\end{array} \xrightarrow[\mathrm{H_2O}]{\text{fast}} 2\mathrm{Ni^{III}(CN)_4(H_2O)_2^-} + \begin{array}{c}\mathrm{Cl^-} \\ \text{or} \\ \mathrm{OH^-}\end{array}$$

An alternative mechanism based on a one-electron reaction of the chlorine species in the rate-determining step is given in Scheme III. For the $\mathrm{Cl_2}$ pathway, either $^\bullet\mathrm{Cl}$ or $\mathrm{Cl_2^-}$ may form as intermediates. A similar mechanism is proposed for the oxidation of $\mathrm{Fe^{II}(CN)_6^{4-}}$ by HOCl, where $k_{\mathrm{HOCl}} = 4.7 \times 10^{-2}$ $\mathrm{M^{-1}\ s^{-1}}$ ($\mu = 1.0$ M, 25 °C).[36] The $\mathrm{Fe^{II}(CN)_6^{4-}}$ complex is coordinately saturated, which prevents it from undergoing an oxidative-addition reaction such as that listed in Scheme II. However, $\mathrm{Ni^{II}(CN)_4^{2-}}$ has two open coordination sites suitable for oxidative addition.

Both the one- and two-electron-oxidation mechanisms are plausible, but the two-electron process is more favorable thermodynamically. Estimated potentials at $\mathrm{p[H^+]}$ 5.00 for both one- and two-electron reductions for the three chlorine oxidants are given in Table VII. The potential for the $\mathrm{Ni^{III,II}(CN)_4(H_2O)_2^{-,2-}}$ couple is 1.15 V (vs NHE).[2] In Scheme III, the first reaction has a large thermodynamic barrier ($\Delta E \simeq -0.72$ to -1.0 V). The

---

(29) Jones, M. M.; Morgan, K. A. *J. Inorg. Nucl. Chem.* **1972**, *34*, 259–279.
(30) Elding, L. I.; Gustafson, L. *Inorg. Chim. Acta* **1976**, *19*, 165–171.
(31) Nag, K.; Chakravorty, A. *Coord. Chem. Rev.* **1980**, *33*, 87–147.
(32) Panda, R. K.; Acharya, S.; Neogi, N.; Ramaswamy, D. *J. Chem. Soc., Dalton Trans.* **1983**, 1225–1231.
(33) Moharty, J. G.; Singh, R. P.; Chakravorty, A. *Inorg. Chem.* **1979**, *14*, 2178–2184.
(34) McCartney, D. H.; McAuley, A. *Can. J. Chem.* **1983**, *61*, 103–108.
(35) Lappin, A. G.; Osvath, P.; Baral, S. *Inorg. Chem.* **1987**, *26*, 3089–3094.
(36) Hin-Fat, L. *J. Chem. Soc., Dalton Trans.* **1988**, 273–275.

Scheme III. Parallel Pathways with •Cl Radical Intermediates

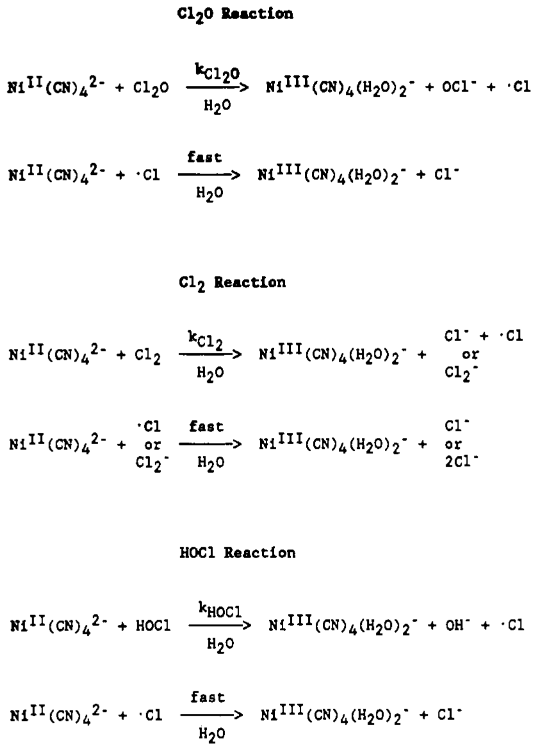

$$Ni^{II}(CN)_4^{2-} + Cl_2O \xrightarrow[H_2O]{k_{Cl_2O}} Ni^{III}(CN)_4(H_2O)_2^- + OCl^- + \cdot Cl$$

$$Ni^{II}(CN)_4^{2-} + \cdot Cl \xrightarrow[H_2O]{fast} Ni^{III}(CN)_4(H_2O)_2^- + Cl^-$$

$$Ni^{II}(CN)_4^{2-} + Cl_2 \xrightarrow[H_2O]{k_{Cl_2}} Ni^{III}(CN)_4(H_2O)_2^- + \begin{matrix} Cl^- + \cdot Cl \\ or \\ Cl_2^- \end{matrix}$$

$$Ni^{II}(CN)_4^{2-} + \begin{matrix} \cdot Cl \\ or \\ Cl_2^- \end{matrix} \xrightarrow[H_2O]{fast} Ni^{III}(CN)_4(H_2O)_2^- + \begin{matrix} Cl^- \\ or \\ 2Cl^- \end{matrix}$$

$$Ni^{II}(CN)_4^{2-} + HOCl \xrightarrow[H_2O]{k_{HOCl}} Ni^{III}(CN)_4(H_2O)_2^- + OH^- + \cdot Cl$$

$$Ni^{II}(CN)_4^{2-} + \cdot Cl \xrightarrow[H_2O]{fast} Ni^{III}(CN)_4(H_2O)_2^- + Cl^-$$

Table VII. Estimated Reduction Potentials of Chlorine Oxidants at p[H$^+$] 5.00[a]

couple	$E°$, V (vs NHE)
$Cl_2O + H_2O + 2e^- = HOCl + OH^- + Cl^-$	1.4
$Cl_2 + 2e^- = 2Cl^-$	1.36
$HOCl + 2e^- = OH^- + Cl^-$	1.35
$Cl_2O + H_2O + e^- = HOCl + OH^- + \cdot Cl$	0.13
$Cl_2 + e^- = Cl^- + \cdot Cl$	0.23
$Cl_2 + e^- = Cl_2^-$	0.43
$HOCl + e^- = OH^- + \cdot Cl$	0.13

[a] 1 M chlorine species; 25.0 °C. Values are calculated from data obtained in ref 19, 21, and 40 and in: Kozlov, Y. N.; Vorob'eva, T. P.; Purmal, A. P. *Zh. Fiz. Khim.* **1981**, *55*, 2279–2284. Thorton, A. T.; Laurence, G. S. *J. Chem. Soc., Dalton Trans.* **1973**, 1632–1636.

second reaction, which is reduction of a •Cl radical, is very favorable. In contrast, the two-electron-process mechanism (Scheme II) is more appropriate from a thermodynamic perspective. An estimate of the potentials involved for Scheme II can be made with two considerations. First, studies of the decomposition of $Ni^{III}(CN)_4(H_2O)_2^-$ showed no evidence for a nickel(IV) product.[2] Thus, the reaction in eq 22 is unfavorable, which signifies $E°$-

$$2Ni^{III}(CN)_4(H_2O)_2^- \rightarrow Ni^{II}(CN)_4^{2-} + Ni^{IV}(CN)_4(H_2O)_2 \qquad (22)$$

$(Ni^{IV,III}) > 1.15$ V. Second, it is assumed that $E°(Ni^{IV,II}) \leq 1.4$ V for the Cl_2O pathway. This leads to the following limitations in potentials:

$$1.15 < E°(Ni^{IV,III}) \leq 1.6;\ 1.15 < E°(Ni^{IV,II}) \leq 1.4 \qquad (23)$$

Thus, both reactions in Scheme II can be favorable thermodynamically.

The rate-determining step in Scheme II involves an oxidative-addition reaction. This type of reaction is similar to the mechanism for the oxidation of $Pt^{II}(CN)_4^{2-}$ by Cl_2 and HOCl (eqs 1 and 2) proposed by Drougge and Elding.[9] In their studies, a Cl_2O pathway was not observed. This is probably due to a combination of more acidic conditions, lack of buffer, and the presence of Cl^- used in their studies. These conditions make the Cl_2 pathway more favorable. The calculated ratio k_{Cl_2}/k_{HOCl} for oxidation of $Ni^{II}(CN)_4^{2-}$ is very similar to the corresponding ratio for oxidation of $Pt^{II}(CN)_4^{2-}$:

$$k_{Cl_2}/k_{HOCl} \text{ for } Pt^{II}(CN)_4^{2-} = 1 \times 10^5$$

$$k_{Cl_2}/k_{HOCl} \text{ for } Ni^{II}(CN)_4^{2-} = 6 \times 10^5$$

The nearly equivalent ratios for oxidation of both $Pt^{II}(CN)_4^{2-}$ and $Ni^{II}(CN)_4^{2-}$ suggest similar mechanisms may be involved, i.e. a two-electron process or oxidative addition. The individual rates for oxidation of $Pt^{II}(CN)_4^{2-}$ by Cl_2 and HOCl are more rapid than those for oxidation of $Ni^{II}(CN)_4^{2-}$:

$$k_{Pt}/k_{Ni} \text{ for } Cl_2 = 30 \qquad k_{Pt}/k_{Ni} \text{ for HOCl} = 200$$

This may be due to a more favorable thermodynamic driving force for $Pt^{II}(CN)_4^{2-}$ oxidation. Potentials for two-electron oxidations of $Pt^{II}(CN)_4^{2-}$ ($\simeq$-0.9 V)[37] are greater than those expected for similar oxidations of $Ni^{II}(CN)_4^{2-}$ (eq 23).

On the basis of these two arguments (the more thermodynamically favorable two-electron reduction of the chlorine oxidants and the similar k_{Cl_2}/k_{HOCl} ratio for $Pt^{II}(CN)_4^{2-}$ and $Ni^{II}(CN)_4^{2-}$ oxidation), we favor the two-electron-oxidation mechanism (Scheme II) and formation of a nickel(IV) intermediate.

The second reaction in Scheme II involves an electron-transfer reaction between the nickel(IV) intermediate and an additional Ni(II) complex. Since the Ni(II) complex has two open axial positions, we propose the reaction proceeds by an inner-sphere pathway via either a Cl^- (Cl_2O, Cl_2, and HOCl) or a OH^- bridge (HOCl). Both OH^- and Cl^- are effective bridging groups that can facilitate electron transfer.[38] Such enhancement is observed in electron-transfer reactions with nickel(II,III) peptide complexes.[39] The final product is $Ni^{III}(CN)_4(H_2O)_2^-$, because the axial groups are sufficiently labile to enable rapid substitution of water molecules.

The studies by Drougge and Elding of $Pt^{II}(CN)_4^{2-}$ oxidation reactions also showed evidence for a OCl^- pathway, where k_{OCl} is estimated to be 10 $M^{-1}\ s^{-1}$.[9] We did not observe a OCl^- pathway for the oxidation of $Ni^{II}(CN)_4^{2-}$. At p[H$^+$] 8.9 (borate buffer), where OCl^- is the predominant chlorine species (eq 4), there is no evidence of $Ni^{III}(CN)_4(H_2O)_2^-$ formation with 0.9 mM OCl^- and 2×10^{-5} M $Ni^{II}(CN)_4^{2-}$. Rather, only the decomposition of $Ni^{II}(CN)_4^{2-}$ is evident with OCl^- acting as a scavenger. The decomposition rate is the same magnitude as that determined with I_2 as a scavenger.[4] Lack of evidence for $Ni^{III}(CN)_4(H_2O)_2^-$ formation from OCl^- oxidation of $Ni^{II}(CN)_4^{2-}$ is not surprising since the thermodynamic barrier for the reaction becomes larger at higher p[H$^+$] values (e.g. $E°(OCl^-,Cl^-) \simeq 1.17$ V at p[H$^+$] 9.00[40]). There is also an accelerated decomposition of $Ni^{III}(CN)_4(H_2O)_2^-$ in base, which is caused by OCl^-. This reaction is proposed to be the oxidation of OCl^- to ClO_2^- by $Ni^{III}(CN)_4(H_2O)_2^-$.[2]

Rate Comparisons. The trend in second-order rate constants for the three pathways of $Ni^{II}(CN)_4^{2-}$ oxidation is

$$k_{Cl_2O} \gg k_{Cl_2} \gg k_{HOCl} \qquad (24)$$

The results are summarized in Table VI. The trend in rate constants does not follow the thermodynamic driving force of the reaction as seen by the $E°$ values in Table VII. The rate-determining step in Scheme II can be divided into two steps (eqs 25 and 26). The first step involves the rapid association between the chlorine species and the Ni(II) complex to form a weak precursor complex. The second step involves simultaneous breaking of a Cl–O bond (Cl_2O, HOCl) or a Cl–Cl bond (Cl_2) and Cl^+ or OH^+ transfer (the oxidative-addition step). The rates of these processes may depend on the strengths of these bonds. The bond dissociation energies for Cl–OCl, Cl–Cl,[41] and HO–Cl[42]

---

(37) Goldberg, R. N.; Hepler, L. G. *Chem. Rev.* **1968**, *68*, 229–252.
(38) Haim, A. *Prog. Inorg. Chem.* **1983**, *30*, 273–357.
(39) Murray, C. K.; Margerum, D. W. *Inorg. Chem.* **1983**, *22*, 463–469.
(40) Bard, A. J.; Parsons, R.; Jordon, J. *Standard Potentials in Aqueous Solution*; Marcel Dekker: New York, 1985; pp 70–77.
(41) Darwent, B. *Natl. Stand. Ref. Data Ser.* (*U.S. Natl. Bur. Stand.*) **1970**, *NSRDS-NBS 31*.
(42) Kerr, J. C. *Chem. Rev.* **1966**, *66*, 465–500.

$$Ni^{II}(CN)_4{}^{2-} + \begin{array}{c} Cl_2O \\ Cl_2 \\ HOCl \end{array} \rightleftarrows \begin{array}{c} [Ni^{II}(CN)_4(Cl_2O)]^{2-} \\ [Ni^{II}(CN)_4(Cl_2)]^{2-} \\ [Ni^{II}(CN)_4(HOCl)]^{2-} \end{array} \qquad (25)$$

$$\begin{array}{c} [Ni^{II}(CN)_4(Cl_2O)]^{2-} \\ [Ni^{II}(CN)_4(Cl_2)]^{2-} \end{array} \xrightarrow{H_2O} Ni^{IV}(CN)_4(Cl)(H_2O)^- + \begin{array}{c} OCl^- \\ Cl^- \end{array}$$

$$[Ni^{II}(CN)_4(HOCl)]^{2-} \xrightarrow{H_2O} \begin{array}{c} Ni^{IV}(CN)_4(Cl)(H_2O)^- + OH^- \\ \text{or} \\ Ni^{IV}(CN)_4(OH)(H_2O)^- + Cl^- \end{array} \qquad (26)$$

are 143, 244, and 251 kJ mol^{-1} (25.0 °C), respectively. Although these bond energies are for a homolytic cleavage, they provide an approximation of the relative bond strengths for these species. We propose that Cl_2O reacts more rapidly with $Ni^{II}(CN)_4{}^{2-}$ than either Cl_2 or HOCl because of the ease with which it can release Cl^+.

An interesting comparison for the trend in eq 24 can be made with the trend in rates for the oxidation of $Co^{II}L^{2-}$ complexes, where L = $EDTA^{4-}$ or $CyDTA^{4-}$(*trans*-1,2 diaminocyclohexane-*N*,*N*,*N'*,*N'*-tetraacetate), by OBr^-, HOBr, and Br_2:[43,44]

$$OBr^- \gg HOBr \gg Br_2 \qquad (27)$$

These reactions are postulated to proceed by an inner-sphere electron-transfer mechanism that takes place with formation of radical intermediates, i.e. one-electron steps. Thus, there is no relation between the homolytic bond energies for the various bromine species and the trend observed in eq 27. Such a trend would be expected for an atom-transfer mechanism. For oxidation of $Ni^{II}(CN)_4{}^{2-}$ by various chlorine species, the rate constants agree with such a trend, which implies the reaction proceeds by an oxidative-addition or atom-transfer mechanism.

Conclusions

Oxidation of $Ni^{II}(CN)_4{}^{2-}$ by aqueous chlorine to form *trans*-$Ni^{III}(CN)_4(H_2O)_2{}^-$ proceeds via Cl_2O, Cl_2, and HOCl pathways. Cl_2O oxidizes $Ni^{II}(CN)_4{}^{2-}$ 40 times faster than Cl_2 and 2.5×10^7 times faster than HOCl. The ratio k_{Cl_2}/k_{HOCl} for this system is similar to that for oxidation of $Pt^{II}(CN)_4{}^{2-}$, which gives a platinum(IV) product.[9] This and thermodynamic considerations for the first step in the oxidation process suggest the three pathways proceed through formation of a highly reactive nickel(IV) intermediate.

Of the three pathways, the Cl_2O reaction is unique. Cl_2O has been shown to be an active chlorinating agent with a variety of organic reagents.[19,45] However, to our knowledge this is the first time Cl_2O has been shown to be active in the oxidation of a metal-ligand complex in aqueous solution. It is an extremely effective oxidizing agent.

Acetic acid catalysis of Cl_2O formation from HOCl is confirmed, and the catalytic effect is even greater than previously observed.[23] The apparent rapid formation of Cl_2O from Cl_2 and HOCl in the presence of acetic acid merits additional study.

Acknowledgment. This work was supported by National Science Foundation Grant CHE-8720318.

---

(43) Woodruff, W. H.; Margerum, D. W.; Milano, M. J.; Pardue, H. L.; Santini, R. E. *Inorg. Chem.* **1973**, *12*, 1490–1494.

(44) Woodruff, W. H.; Burke, B. A.; Margerum, D. W. *Inorg. Chem.* **1974**, *13*, 2573–2575.

(45) Voudrias, E. A.; Reinhard, M. *Environ. Sci. Technol.* **1988**, *22*, 1049–1056.

Contribution from the Department of Chemistry, Cleveland State University, Cleveland, Ohio 44115,
and Department of Chemistry and Laboratory for Molecular Structure and Bonding,
Texas A&M University, College Station, Texas 77843

Metal–Metal Bonds Involving Vanadium Atoms. A Facile Synthesis of a Novel Divanadium Tetrakis(dithioacetate) That Contains Two μ-η^2-S_2 Bridges from Bis(benzene)vanadium(0) and Dithioacetic Acid

Stan A. Duraj,*[,†] Maria T. Andras,[†] and Piotr A. Kibala[‡]

Received October 4, 1989

The reaction between bis(benzene)vanadium(0), $(\eta^6\text{-}C_6H_6)_2V$, and dithioacetic acid, CH_3CSSH, furnishes a novel dimer, $(CH_3CS_2)_2V(\mu\text{-}\eta^2\text{-}S_2)_2V(S_2CCH_3)_2$, in 56–62% yields. The brown product has been characterized by elemental analyses, NMR, IR, and mass spectrometry, magnetic susceptibility measurements, and X-ray crystallography. The immediate coordination sphere of the two vanadium cores is best regarded as consisting of two distorted trigonal prisms that share the four sulfur atoms that form one rectangular face and have each of the other four rectangular faces capped by one sulfur atom. Because the new compound is diamagnetic and the V–V distance equals 2.800 (2) Å, a single metal–metal bond is postulated for this vanadium–vanadium d^1–d^1 pair. Therefore, each vanadium center has an unusual and rare nine-coordinate geometry, having the form of a tricapped trigonal prism. The compound crystallizes in space group $P2_1/c$ with a = 10.425 (2) Å, b = 11.123 (2) Å, c = 9.133 (4) Å, β = 97.12 (2)°, V = 1051 (1) Å^3, Z = 2, R = 0.0476, and R_w = 0.0598. Other important structural features: the S–S distance of the μ-η^2-S_2 bridge is 1.997 (3) Å, and the V–S distances range from 2.366 (3) to 2.502 (2) Å.

Introduction

With the recognition that metal atoms form direct bonds, the preparation, structural characterization, and reactivity of transition-metal compounds containing M-to-M bonds have become areas of intense study.[1] In contrast to numerous, well-known dinuclear tetracarboxylates possessing quadruple M-to-M bonds such as $M_2(\mu\text{-}O_2CR)_4L_2$ (M = Cr, Mo, W; R = alkyl or aryl groups; L = σ-donor ligands, e.g., H_2O, THF, etc.),[2] as well as dithio analogues of the type $Mo_2(\mu\text{-}S_2CR)_4L_2$ (R = CH_3, C_6H_5; L = THF),[3] similar compounds (that would contain M-to-M bonds

---

[†] Cleveland State University.

[‡] Texas A&M University.

(1) Cotton, F. A.; Walton, R. A. *Multiple Bonds Between Metal Atoms*; Wiley: New York, 1982. Cotton, F. A.; Walton, R. A. *Struct. Bonding (Berlin)* **1985**, *62*, 1. Chisholm, M. H.; Rothwell, I. P. *Prog. Inorg. Chem.* **1982**, *29*, 1. Chisholm, M. H. *Recent Advances in the Chemistry of Metal-Metal Multiple Bonds*; Polyhedron Symposia-in-Print, Vol. 6, No. 4; Pergamon: Oxford, U.K., 1987. See also Figures 9–11 in: Cotton, F. A. *J. Chem. Educ.* **1983**, *60*, 713.

(2) Cotton, F. A.; Wilkinson, G. *Advanced Inorganic Chemistry*; Wiley: New York, 1988.

0020-1669/90/1329-1232$02.50/0